

Viewing the noise propagation mechanism in a unidirectional transition cascade from the perspective of stability

Qi-Ming Pei(裴启明), Bin-Qian Zhou(周彬倩), Yi-Fan Zhou(周祎凡), Charles Omotomide Apata, and Long Jiang(蒋龙)

Citation: Chin. Phys. B, 2021, 30 (**11**): 118704. DOI: 10.1088/1674-1056/ac0ee7
Journal homepage: http://cpb.iphy.ac.cn; http://iopscience.iop.org/cpb

What follows is a list of articles you may be interested in

Magnetic-resonance image segmentation based on improved variable weight multi-resolution Markov random field in undecimated complex wavelet domain

Hong Fan(范虹), Yiman Sun(孙一曼), Xiaojuan Zhang(张效娟), Chengcheng Zhang(张程程), Xiangjun Li(李向军), and Yi Wang(王乙)

Chin. Phys. B, 2021, 30 (**7**): 078703. DOI: 10.1088/1674-1056/abe1a2

Relationship between manifold smoothness and adversarial vulnerability in deep learning with local errors

Zijian Jiang(蒋子健), Jianwen Zhou(周健文), and Haiping Huang(黄海平)

Chin. Phys. B, 2021, 30 (**4**): 048702. DOI: 10.1088/1674-1056/abd68e

Effective suppression of beta oscillation in Parkinsonian state via a noisy direct delayed feedback control scheme

Hai-Tao Yu(于海涛), Zi-Han Meng(孟紫寒), Chen Liu(刘晨), Jiang Wang(王江), and Jing Liu(刘静)

Chin. Phys. B, 2021, 30 (**3**): 038703. DOI: 10.1088/1674-1056/abd395

Identification of denatured and normal biological tissues based on compressed sensing and refined composite multi-scale fuzzy entropy during high intensity focused ultrasound treatment

Shang-Qu Yan(颜上取), Han Zhang(张含), Bei Liu(刘备), Hao Tang(汤昊), and Sheng-You Qian(钱盛友)

Chin. Phys. B, 2021, 30 (**2**): 028704. DOI: 10.1088/1674-1056/abcfa7

Dynamics and coherence resonance in a thermosensitive neuron driven by photocurrent

Ying Xu(徐莹), Minghua Liu(刘明华), Zhigang Zhu(朱志刚), Jun Ma(马军)

Chin. Phys. B, 2020, 29 (**9**): 098704. DOI: 10.1088/1674-1056/ab9dee

---

Viewing the noise propagation mechanism in a unidirectional transition cascade from the perspective of stability*

Qi-Ming Pei(裴启明)†, Bin-Qian Zhou(周彬倩), Yi-Fan Zhou(周祎凡), Charles Omotomide Apata, and Long Jiang(蒋龙)‡

School of Physics and Optoelectronic Engineering, Yangtze University, Jingzhou 434023, *China*

(Received 15 April 2021; revised manuscript received 25 May 2021; accepted manuscript online 28 June 2021)

Noise and noise propagation are inevitable and play a constructive role in various biological processes. The stability of cell homeostasis is also a critical issue. In the unidirectional transition cascade of colon cells, stem cells (SCs) are the source. They differentiate into transit-amplifying cells (TACs), and TACs differentiate into fully differentiated cells (FDCs). Two differentiation processes are irreversible. The stability factor is introduced so that the noise propagation mechanism from the perspective of stability is studied according to the noise propagation formulas. It is found that the value of the stability factor corresponding to the minimum noise in FDCs may be the best choice to enable colon cells to maintain high stability and low noise of the cascade. Moreover, for the source cell, the total noise only includes intrinsic noise; for the downstream cell with self-proliferation capability, the total noise mainly depends on its intrinsic noise and transmitted noise from upstream cells, and its intrinsic noise is dominant. For the downstream cell without self-proliferation capability, the total noise is mainly determined by transmitted noises from upstream cells, and there is a minimum value. This work provides a new approach for studying the mechanism of noise propagation while considering the stability of cell homeostasis in biological systems.

Keywords: noise, noise propagation, stability, linear approximation

PACS: 87.18.Tt, 05.45.−a, 05.10.Gg, 02.50.−r **DOI:** 10.1088/1674-1056/ac0ee7

1. Introduction

Noise is unavoidable and permeates into all levels of biological systems.[1–3] It includes intrinsic noise generated by random biochemical reactions and external noise arising from changes in the microenvironment.

Noise plays a constructive role in key cellular activities. It is beneficial to metabolism, development, the cell cycle, circadian rhythms, aging, and so on.[4,5] The noised-induced stochastic alternation between the focus and the limit cycle will result in a synchronized early after-depolarization-like rhythm.[6] Driven by noise, some spatiotemporal dynamic behavior (such as synchronization, spiral waves, spatial periodicity, and time sequences) will appear, thereby affecting the brain's function.[7]

Recent studies have shown that noise is also important in the propagation of neuroelectric signals.[8–11] In the functional neural circuit that combines a thermistor and a phototube, it is possible to detect coherent resonance by applying Gaussian white noise.[12] The direct delayed feedback control through noise can effectively suppress the beta oscillation in the Parkinson state.[13] From a physical point of view, noise driving will inject energy.[14] Energy can be encoded to adjust the dynamics of nonlinear oscillators and circuits, and can especially cause non-coupling synchronization.[15] In two nonlinear circuits, encoded energy can enhance the dependence of synchronization and dynamics on the initial values.[16,17]

In other cases, noise is deleterious and hence needs to be suppressed.[18] It can reduce biological fitness and cause genetic mutations.[19] In tumor cells, when noise is too large, the instantaneous cell number will greatly deviate from the equilibrium state, which is a potential risk for tumors.

It was confirmed that noise can be propagated. As early as 2005, the propagation of noise in gene networks was observed by measuring the correlation between gene expressions in a single cell.[20] In the process of signal transduction, noise can also propagate with the signal and seriously affect the fitting response.[21] Furthermore, research in 2018 showed that the expression noise coming from one gene can propagate to the growth, metabolism, and expression of all other genes.[22] At the cellular level, noise can propagate from upstream cells to downstream cells in the colonic cells cascade, and the transmitted noise has an important influence on the total noise in downstream cells.[23,24]

Stability analysis is another key issue in the fields of systems, control, and signal processing.[25] It is an important tool for studying the dynamic behavior of nonlinear systems. In the mathematical model of physical processes, only its stable solutions correspond to the motions that are observed in nature.[26] The high stability of physical properties of the equipment is the goal we have been pursuing, such as thin-

*Project supported by the National Natural Science Foundation of China (Grant No. 11605014).

†Corresponding author. E-mail: qmpei@yangtzeu.edu.cn

‡Corresponding author. E-mail: jianglong@yangtzeu.edu.cn

© 2021 Chinese Physical Society and IOP Publishing Ltd

film photonic devices,[27] optical atomic clocks,[28] and perovskite thermoelectric devices.[29] However, sometimes instability is also very important. For example, the nonlinear growth of hydrodynamic instabilities will lead to the degradation of inertial confinement fusion implosion.[30] The instability of Richtmyer–Meshkov is a key factor in the rupture and atomization of liquid films caused by shock waves.[31]

Recently, stability analysis has become a hot and promising research topic.[32] It can provide some suggestions not only for the control of rumor propagation or virus transmission, but also for the clinical treatment of diseases. For example, stability analysis of a SAIR rumor-spreading model was used to discuss the optimal control strategy for reducing the frequency of rumor propagation.[33] Stability analysis and numerical simulation of the SEIR model on COVID-19 transmission provided some references for early prevention of the spread of COVID-19 in Indonesia.[34] Through stability analysis of a fractional HIV-AIDS epidemic model with memory and general incidence rate, an optimal strategy to minimize the spread of the disease in the population can be determined.[35] Stability analysis and numerical simulation of a HPV infection model with early-stage cervical cancer showed that the optimal control of HPV infection can reduce the resulting cancer cells.[36]

Then, interesting questions arise. For a unidirectional phenotypic transition cascade, how does one study the noise properties while maintaining a steady equilibrium state? What is the mechanism of noise propagation from the perspective of stability? To address these issues, we choose a three-compartment model of a colonic crypt[37,38] as an example of a stochastic computation system. Instead of the nonlinear dynamic evolution method[39,40] and the linear stability analysis method,[41] the analytical solution of the Langevin equation with elasticity factors[42–44] is used for discussion. From the normalized fluctuation–dissipation relationship, noise propagation formulas are obtained. Through the simulation of these theoretical formulas, the noise propagation mechanism from the stability viewpoint is studied.

In our work, all data are compared with those of the Gillespie algorithm,[45,46] which is a classic approach for stochastic simulation of chemical systems.[47] It is usually used to test whether theoretical results are correct, because this algorithm can give statistically accurate simulations.

This paper is organized as follows. In Section 2, a phenotypic transition cascade in a colonic crypt with coupled saturation and linear feedback is constructed. In Section 3, theoretical formulas with an elasticity factor for noise propagation are derived. The influence of the stability factor of cell equilibrium on noise and noise propagation is studied in Section 4. We end with conclusions and discussions in Section 5.

2. Transition cascade in a colonic crypt with coupled saturation and linear feedbacks

2.1. Model

In the three-compartment model of a colonic crypt,[37] stem cells (SCs) are the source and can differentiate into transit-amplifying cells (TACs), and then TACs can continuously differentiate into fully differentiated cells (FDCs), while two differentiates are irreversible, as shown in Fig. 1. The differentiation probability from SCs to TACs per unit time is α_{12}, and that from TACs to FDCs is α_{23}. SCs and TACs can self-proliferate, and the self-proliferation probabilities per unit time are a_1 and a_2, respectively. FDCs can neither self-proliferate nor differentiate. The three compartments can experience procedural death and be removed from the crypt. The corresponding probabilities per unit time are b_1, b_2, and b_3, respectively.

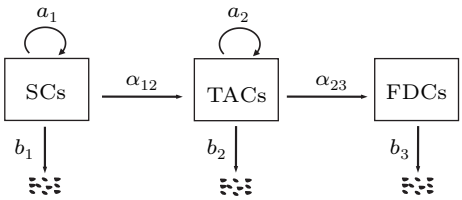


Fig. 1. A schematic diagram of the three compartments in a colonic crypt,[37] in which SCs can differentiate into TACs and TACs can differentiate into FDCs. Here, a_1 and a_2 are the self-proliferation probabilities per unit time of SCs and TACs, respectively, while b_1, b_2, and b_3 are the programmed death probabilities per unit time of each compartment. Here, α_{12} and α_{23} are the differentiation probabilities per unit time from SCs to TACs, and from TACs to FDCs, respectively. To maintain cell populations in homeostasis, α_{12} is regulated by saturation feedback; α_{23} is regulated by linear feedback.

Taking N_i ($i = 1, 2, 3$) as the numbers of SCs, TACs, and FDCs, respectively, the time evolution equation of the cell populations is

$$\frac{\mathrm{d}N_1}{\mathrm{d}t} = a_1 N_1 - b_1 N_1 - \alpha_{12} N_1, \tag{1}$$

$$\frac{\mathrm{d}N_2}{\mathrm{d}t} = a_2 N_2 - b_2 N_2 + \alpha_{12} N_1 - \alpha_{23} N_2, \tag{2}$$

$$\frac{\mathrm{d}N_3}{\mathrm{d}t} = -b_3 N_3 + \alpha_{23} N_2. \tag{3}$$

If all the reaction probabilities are constant, then the three cells will either die instantly or grow to infinity immediately, neither of which conforms to the normal human physiological state. To keep cell populations in homeostasis, linear feedback and saturation feedback were introduced to regulate the differentiation rate.[46] In linear feedback, the cell differentiation rate increases linearly with the increase in its population, and there is no upper limit. Linear feedback is strong enough to prevent any unlimited growth of three cell populations. In saturation feedback, although the differentiation rate also increases with the increase in its population, it will reach a maximum instead of increasing indefinitely. Saturation feedback can help ex-

plain the presence of benign tumors or adenomas before carcinogenesis occurs. Rather than a single and identical feedback, the coupled saturation and linear feedbacks are considered in this paper: that is, the differentiation rate of SCs is regulated by saturation feedback, and that of TACs is regulated by linear feedback. Thus, $\alpha_{12} = \alpha_{10} + (k_1 N_1)/(1 + m_1 N_1)$, $\alpha_{23} = \alpha_{20} + k_2 N_2$, in which α_{10} and α_{20} are an inherent differentiation rate of SCs and TACs, respectively. Here, k_i ($i = 1$, 2) represents the speed of the feedback response, and m_1 represents the feedback saturation of SCs. Some studies have shown that this coupled feedback is more suitable for explaining tumor development.

2.2. Steady states

Taking $\mathrm{d}N_i/\mathrm{d}t = 0$, then the steady states N_i^{s} are obtained as

$$\begin{aligned} N_1^{\mathrm{s}} &= \frac{\eta_1}{k_1 - m_1\eta_1}, \\ N_2^{\mathrm{s}} &= \frac{\eta_2 + \sqrt{\eta_2^2 + 4\chi k_2}}{2k_2}, \\ N_3^{\mathrm{s}} &= \frac{\alpha_{23}}{b_3} N_2^{\mathrm{s}}. \end{aligned} \tag{4}$$

Here, $\eta_1 = a_1 - b_1 - \alpha_{10}$ and $\eta_2 = a_2 - b_2 - \alpha_{20}$ denote the inherent net growth rates of SCs and TACs, respectively. And $\chi = \alpha_{12} N_1^{\mathrm{s}}$ is the differentiation rate of SCs at the steady state. Since the number of each cell population in the steady state is positive, η_1 should satisfy the following conditions:

$$0 < \eta_1 < \frac{k_1}{m_1}. \tag{5}$$

2.3. The elasticity

To qualitatively describe how phenotype k affects the balance between elimination and production of phenotype i, the elasticity H_{ki} (i, $k = 1$, 2, 3) is introduced, which is defined as[42]

$$H_{ki} = \left\langle \frac{\partial \ln\left(J_i^- / J_i^+\right)}{\partial \ln N_k} \right\rangle = \left\langle \frac{N_k}{J_i^+} \frac{\partial}{\partial N_k} \left(J_i^- - J_i^+\right) \right\rangle, \tag{6}$$

where $J_i^+ = a_i N_i + \sum_{j \neq i} \alpha_{ji} N_j$, $J_i^- = b_i N_i + \sum_{j \neq i} \alpha_{ij} N_i$, indicating the pure production rate and the pure elimination rate, respectively. The angled bracket "$\langle\ \rangle$" indicates that one must take the average. The elasticity is also named as the logarithmic gain, sensitivity amplification, or susceptibility.[43,44]

Based on Eqs. (1)–(3), it is easy to get

$$H_{13} = H_{21} = H_{31} = H_{32} = 0, \tag{7}$$

$$H_{33} = 1, \tag{8}$$

$$H_{11} = \frac{k_1 \langle N_1 \rangle}{a_1 \left(1 + m_1 \langle N_1 \rangle\right)^2}, \tag{9}$$

$$H_{22} = \frac{1}{b_2 + \alpha_{23}} \left(\frac{\chi}{\langle N_2 \rangle} + k_2 \langle N_2 \rangle \right), \tag{10}$$

$$H_{12} = -\frac{1}{a_2 \langle N_2 \rangle + \chi} \left[\chi + \frac{k_1 \langle N_1 \rangle^2}{\left(1 + m_1 \langle N_1 \rangle\right)^2} \right], \tag{11}$$

$$H_{23} = -\left(1 + \frac{k_2 \langle N_2 \rangle}{\alpha_{23}}\right). \tag{12}$$

It can be seen that $H_{11}, H_{22} > 0$ and $H_{12}, H_{23} < 0$ because $\langle N_i \rangle$ and the parameters are all positive. So, for SCs and TACs, the impact on their self-elimination is greater than that on their self-production. And upstream cells have a greater influence on the production of downstream cells than on their elimination. This is because, regardless of whether linear feedback or saturated feedback acts on cell differentiation, it can promote their own elimination, thereby generating more downstream cells.

In this sense, the elasticity H_{ki} can be understood as the regulation intensity.

2.4. Langevin equation

By linearizing Eqs. (1)–(3) near the steady state,[48] Langevin equations[49,50] can be obtained as

$$\begin{aligned} \frac{\mathrm{d}x_i}{\mathrm{d}t} &= -\frac{x_i}{\tau_i} \sum_{j=1}^{3} H_{ji} + \xi_i(t) \\ &\equiv -\frac{x_i}{\tau_i} \mathcal{H}_i + \xi_i(t), \quad i = 1, 2, 3. \end{aligned} \tag{13}$$

Here, $x_i = N_i - \langle N_i \rangle$ is a deviation from the steady state, $\xi_i(t)$ is a Gaussian white noise, τ_i is the average lifetime of phenotype i, which is defined as the average number $\langle N_i \rangle$ divided by its average rate of elimination $\langle J_i^- \rangle$. Under the steady state, $\langle J_i^- \rangle = \langle J_i^+ \rangle = \langle J_i \rangle$, then $\tau_i = \langle N_i / J_i^- \rangle = \langle N_i / J_i^+ \rangle = \langle N_i / J_i \rangle$. According to Eqs. (1)–(3), the average lifetimes of SCs, TACs, and FDCs in a colonic crypt are, respectively,

$$\tau_1 = 1/a_1, \quad \tau_2 = 1/(b_2 + \alpha_{23}), \quad \tau_3 = 1/b_3. \tag{14}$$

And $\mathcal{H}_i \equiv \sum_{j=1}^{3} H_{ji}$ is the total regulation intensity of phenotype i, describing the influence of all phenotypes (including itself) in the cascade on the phenotype i. According to Eqs. (7)–(12), it is easy to obtain

$$\mathcal{H}_1 = H_{11}, \quad \mathcal{H}_2 = H_{12} + H_{22}, \quad \mathcal{H}_3 = H_{23} + H_{33}. \tag{15}$$

Solving Eq. (13), we can get

$$x_i = \exp\left(-\mathcal{H}_i t / \tau_i\right) \begin{cases} \text{stable}, & \text{if } \mathcal{H}_i > 0, \\ \text{unstable}, & \text{if } \mathcal{H}_i < 0. \end{cases} \tag{16}$$

The deviation x_1 will change exponentially with $\left(-\mathcal{H}_i t / \tau_i\right)$. Since $\tau_1 > 0$, the monotonicity or stability of the curve is uniquely determined by $\mathcal{H}_i$. When $\mathcal{H}_i > 0$, the equilibrium of phenotype i is stable, otherwise, it will be unstable.

As the source of the cascade, SCs will not be affected by downstream cells, so its stability equilibrium condition is only determined by H_{11}. Because downstream cells will be affected

by upstream cells, their stability conditions are related to upstream cells. For example, both H_{22} and H_{12} jointly determine the stability conditions of TACs' equilibrium, and H_{33} and H_{23} together determine the stability conditions of FDCs' equilibrium, see Eq. (15). When $\mathcal{H}_1 = H_{11} > 0$, $\mathcal{H}_2 = H_{22} + H_{12} > 0$, and $\mathcal{H}_3 = H_{33} + H_{23} > 0$, SCs, TACs and FDCs are in a stable equilibrium state, respectively. Otherwise, they will be in an unstable equilibrium state: that is, once SCs, TACs, or FDCs are disturbed, they will be far from the equilibrium state.

In this sense, the total regulation intensity H_i can also be interpreted as a stability factor of cell equilibrium, which is used to judge whether the cell can return to its original equilibrium state after being disturbed.

3. Noise propagation formulas

In stochastic dynamics theory, the master equation gives the joint probability distribution of population dynamics.[49] Although the master equation cannot be solved, it can be expanded using van Kampen's Ω-expansion method to obtain the linear Fokker–Planck equation.[50] In the steady state, the coefficients of the Fokker–Planck equation will satisfy the fluctuation–dissipation relationship. To facilitate discussion, the fluctuation–dissipation relationship should be normalized[23,24] to

$$\boldsymbol{M}\boldsymbol{V} + (\boldsymbol{M}\boldsymbol{V})^{\mathrm{T}} + \boldsymbol{D} = 0, \tag{17}$$

in which $\boldsymbol{M}$ is the normalized drift matrix, and is related to the elasticity H_{ki} and average lifetime τ_i by

$$M_{ik} = -\frac{H_{ki}}{\tau_i}. \tag{18}$$

$\boldsymbol{D}$ is the normalized diffusion matrix, which can be obtained based on Eqs. (1)–(3) as

$$D_{ii} = \frac{2\left[a_i \langle N_i\rangle + \sum_{j\neq i}\alpha_{ji}\langle N_j\rangle\right]}{\langle N_i\rangle^2}, \tag{19}$$

$$D_{ik} = -\left(\frac{\alpha_{ik}}{\langle N_k\rangle} + \frac{\alpha_{ki}}{\langle N_i\rangle}\right) \quad (k \neq i). \tag{20}$$

$\boldsymbol{V}$ includes normalized variance V_{ii} and normalized covariance V_{ik} $(k \neq i)$. The former characterizes the fluctuation in phenotype i, and the latter represents the degree of correlation between the noise in phenotype i and that in phenotype k.

By expanding Eq. (17) with $V_{ij} = V_{ji}$ $(j \neq i)$, we can get V_{ij} as follows:

$$V_{12} = V_{21} = -V_{11}\frac{H_{12}}{H_{22}}\cdot\frac{\Xi_2}{\Xi_1+\Xi_2} - \frac{\alpha_{12}/\langle N_2\rangle}{\Xi_1+\Xi_2}, \tag{21}$$

$$V_{13} = V_{31} = -V_{12}\frac{H_{23}}{H_{33}}\frac{\Xi_3}{\Xi_1+\Xi_3}, \tag{22}$$

$$V_{23} = V_{32} = -V_{13}\frac{H_{12}}{H_{22}}\cdot\frac{\Xi_2}{\Xi_2+\Xi_3} - V_{22}\frac{H_{23}}{H_{33}}\cdot\frac{\Xi_3}{\Xi_2+\Xi_3} - \frac{\alpha_{23}/\langle N_3\rangle}{\Xi_2+\Xi_3}, \tag{23}$$

with $\Xi_i = H_{ii}/\tau_i = \left\langle \partial\left(J_i^- - J_i^+\right)/\partial N_i\right\rangle$, which is the net average apoptosis probability per unit time, indicating the change rate of the net apoptosis rate with its own population.

Also, we can obtain V_{ii} as follows:

$$V_{11} = \underbrace{\frac{1}{\langle N_1\rangle H_{11}}}_{\text{intrinsic noise in SCs}}, \tag{24}$$

$$V_{22} = \underbrace{\frac{1}{\langle N_2\rangle H_{22}}}_{\text{intrinsic noise in TACs}} + \underbrace{V_{11}\frac{\Xi_2}{\Xi_1+\Xi_2}\cdot\left(\frac{H_{12}}{H_{22}}\right)^2}_{\text{transmitted noise from SCs}} + \underbrace{\frac{\alpha_{12}/\langle N_2\rangle}{\Xi_1+\Xi_2}\cdot\frac{H_{12}}{H_{22}}}_{\text{conversion noise between SCs and TACs}}, \tag{25}$$

$$\begin{aligned} V_{33} = {} & \underbrace{\frac{1}{\langle N_3\rangle H_{33}}}_{\text{intrinsic noise in FDCs}} \\ & + \underbrace{V_{11}\frac{\Xi_2}{\Xi_1+\Xi_2}\cdot\frac{\Xi_2}{\Xi_2+\Xi_3}\cdot\frac{\Xi_3}{\Xi_1+\Xi_3}\cdot\left(\frac{H_{12}}{H_{22}}\right)^2\cdot\left(\frac{H_{23}}{H_{33}}\right)^2}_{\text{transmitted noise from SCs}} \\ & + \underbrace{V_{22}\frac{\Xi_3}{\Xi_2+\Xi_3}\cdot\left(\frac{H_{23}}{H_{33}}\right)^2}_{\text{transmitted noise from TACs}} \\ & + \underbrace{\frac{\Xi_2}{\Xi_2+\Xi_3}\cdot\frac{\Xi_3}{\Xi_1+\Xi_3}\cdot\frac{\alpha_{12}/\langle N_2\rangle}{\Xi_1+\Xi_2}\cdot\frac{H_{12}}{H_{22}}\left(\frac{H_{23}}{H_{33}}\right)^2}_{\text{conversion noise between SCs and TACs}} \\ & + \underbrace{\frac{\alpha_{23}/\langle N_3\rangle}{\Xi_2+\Xi_3}\cdot\frac{H_{23}}{H_{33}}}_{\text{conversion noise between TACs and FDCs}}. \end{aligned} \tag{26}$$

The normalized variation V_{ii} describes the total noise in phenotypic i. The noise decomposition method here is consistent with that in the gene network.[43] The intrinsic noise originates from a small number of cells, transmitted noise is caused by the total noise of upstream cells, and inter-conversion noise comes from the interaction (i.e., differentiation) of cells.

SCs are the sources of this phenotypic transition cascade; they do not have an external fluctuation environment coming from other phenotypes. Therefore, there is only intrinsic noise in SCs, see Eq. (24). In downstream cells, in addition to the intrinsic noise, transmitted noise will be generated due to the external fluctuation environment provided by the upstream cell. Due to the differentiation from upstream cells, there is also inter-conversion noise, see Eqs. (25) and (26). Intrinsic noise

is inversely proportional to the product of its average $\langle N_i \rangle$ and self-elasticity H_{ii}. The transmitted noise depends on the total noise of upstream phenotypes V_{ii}, the elasticity H_{ki}, and the net average apoptosis probability Ξ_i. The inter-conversion noise is determined by the differentiation rate $\alpha_{i,i+1}$ $(i = 1, 2)$, H_{ki}, and Ξ_i. From Eq. (26), we also find the noise in SCs can propagate to FDCs, even if SCs cannot directly differentiate to FDCs. Moreover, the noise in the downstream phenotype can be expressed as a linear function of the noise in the upstream phenotypes. That is, the contribution of upstream phenotypic fluctuations to downstream phenotypic fluctuations is additive.

4. Simulations and results

4.1. The characteristics of the stability factor

From Eq. (4), we find that both the inherent net growth rate of SCs η_1 and the feedback response speed k_1 determine the steady state of SCs $N_1^{\rm s}$, thereby affecting the other two steady states. Moreover, η_1 is the key parameter.[37] So, we choose η_1 as the control variable. And a_1 will vary with η_1 due to $a_1 = \eta_1 + b_1 + \alpha_{10}$. The other parameters are $a_2 = 0.5$, $b_1 = 0.1$, $b_2 = 0.1$, $b_3 = 0.323$, $\alpha_{10} = 0.1$, $\alpha_{20} = 0.2$, $k_1 = 0.1$, $m_1 = 0.1$, and $k_2 = 0.01$.[32,33] In this paper, the dimensionless parameters are used.

The steady states $N_i^{\rm s}$ as a function of η_1 are given in Fig. 2. Herein, η_1 changes in the range [0.3, 1]. It is found that when $\eta_1 < 0.8$, the steady states of three populations increase approximately linearly with the increase in η_1, and the changes are relatively gentle. Once $\eta_1 > 0.8$, they will increase rapidly and quickly reach infinity. FDCs increase the fastest, followed by SCs, and TACs increase the slowest.

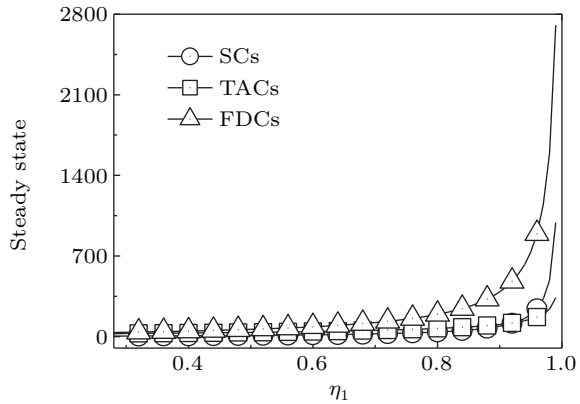


Fig. 2. Steady states $N_i^{\rm s}$ $(i = 1, 2, 3)$ versus SCs inherent net growth rate η_1. The lines are theoretical predictions according to Eq. (4). Other parameter values are given in the text. All the parameters are measured in hour^{-1}.

In the mean field theory, the mean value can be replaced by its stationary population number, namely $\langle N_i \rangle = N_i^{\rm s}$. According to Eqs. (7)–(12), $\mathcal{H}_i$ as a function of η_1 are given in Fig. 3.

It can be seen that $\mathcal{H}_1 > 0$ and $\mathcal{H}_2 > 0$, then SCs and TACs are in a stable equilibrium state. In other words, due to the disturbance $\xi_1(t)$ or $\xi_2(t)$, even if SCs or TACs deviate from the equilibrium state instantaneously, they will return to the original state. However, $\mathcal{H}_3 < 0$, that is, FDCs are in an unstable equilibrium state. Therefore, in colonic crypts, FDCs are most likely to induce colon cancer. Once FDCs are disturbed, they will quickly grow to infinity.

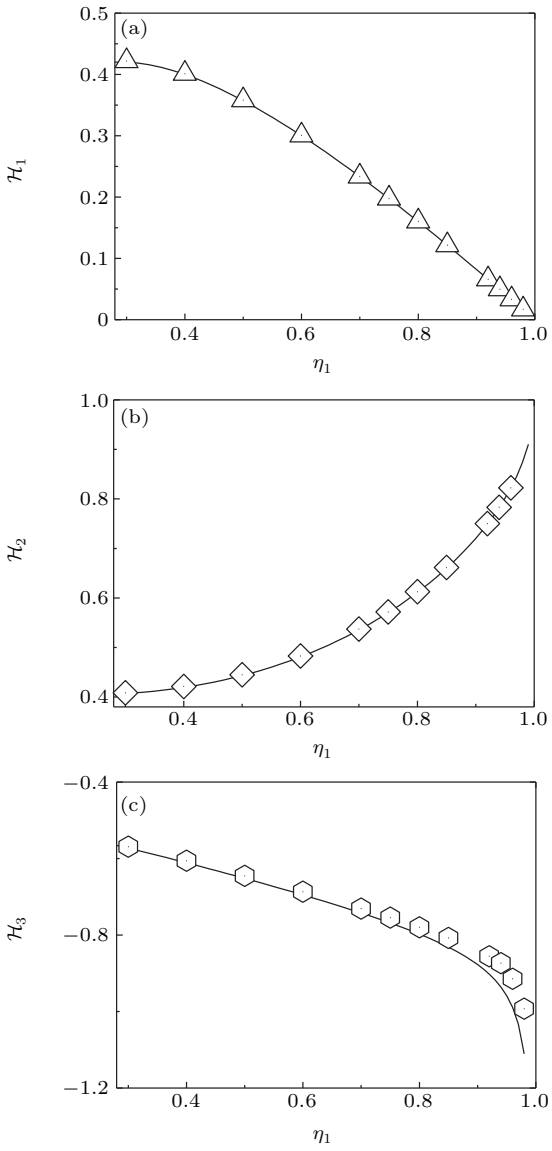


Fig. 3. The stability factor $\mathcal{H}_i$ $(i = 1, 2, 3)$ versus SCs inherent net growth rate η_1. The lines are theoretical predictions according to Eqs. (7)–(12). Hollow markers are from simulations using the Gillespie method.[45,46] Other parameter values are given in the text. All the parameters are measured in hour^{-1}.

From Fig. 3(a), we find $\mathcal{H}_1$ will decrease with the increase in η_1. So, the larger the parameter η_1, the smaller the regulation intensity $\mathcal{H}_1$, and the more difficult it will be to control the stability of SCs. In contrast, $\mathcal{H}_2$ will increase with the increase in η_1, see Fig. 3(b). Then, the larger the parameter η_1, the larger the regulation intensity $\mathcal{H}_2$, and the easier it will be to control the stability of TACs. From Fig. 3(c), it can be found that $\mathcal{H}_3$ will also decrease with the increase in η_1, whereas, $\mathcal{H}_3 < 0$; therefore, the larger the parameter η_1, the smaller the regulation intensity $\mathcal{H}_3$, and the greater the degree of instability of the FDCs' equilibrium.

In short, when $\mathcal{H}_1$, $\mathcal{H}_2$, and $\mathcal{H}_3$ are large, the homeostasis among the three cells is easy to maintain, see Table 1.

Table 1. The stability characteristics of the three cells.

Cell	Value of $\mathcal{H}_i$	Stability	Characteristics
SCs	$\mathcal{H}_1 > 0$	stable	larger $\mathcal{H}_1$, larger regulation intensity, more stable.
TACs	$\mathcal{H}_2 > 0$	stable	larger $\mathcal{H}_2$, larger regulation intensity, more stable.
FDCs	$\mathcal{H}_3 < 0$	unstable	larger $\mathcal{H}_3$, larger regulation intensity, less unstable.

4.2. Effects of the stability factor on the normalized covariance

Based on Eqs. (21)–(23), the normalized covariance $V_{ij} = V_{ji}$ $(i, j = 1, 2, 3;\ j \neq i)$ as a function of H_i is given in Fig. 4. All analytical predictions are in accord with numerical simulations by the Gillespie stochastic algorithm.

It is shown that V_{12}, V_{23}, $V_{13} > 0$. Therefore, any two fluctuations in the three cell populations are positively correlated. In colon cells, downstream cells are mainly produced by the differentiation of upstream cells, so downstream cells will change synchronously with upstream cells. In addition, although there is no direct interaction between SCs and FDCs, the correlation between the two fluctuations of SCs and FDCs is positive. That is, the correlation can be transmitted from SCs to FDCs through TACs. Moreover, V_{13} has an effect on the correlation between TACs and FDCs V_{23}, see Eq. (23).

By comparing the upper layer figures, we find that the covariance V_{12} is a monotonically increasing function of the stability factor $\mathcal{H}_1$ or $\mathcal{H}_3$, whereas, it is a monotonically decreasing function of $\mathcal{H}_2$. So, the correlation between SCs and TACs will be strengthened with the increase in $\mathcal{H}_1$ or $\mathcal{H}_3$, and it will be weakened with the increase in $\mathcal{H}_2$.

The middle and bottom layer figures show that all curves of V_{23} and V_{13} are asymmetric parabolas opening upwards. Therefore, for some optimal total regulation intensities, there is always a minimum value for V_{23} and V_{13}.

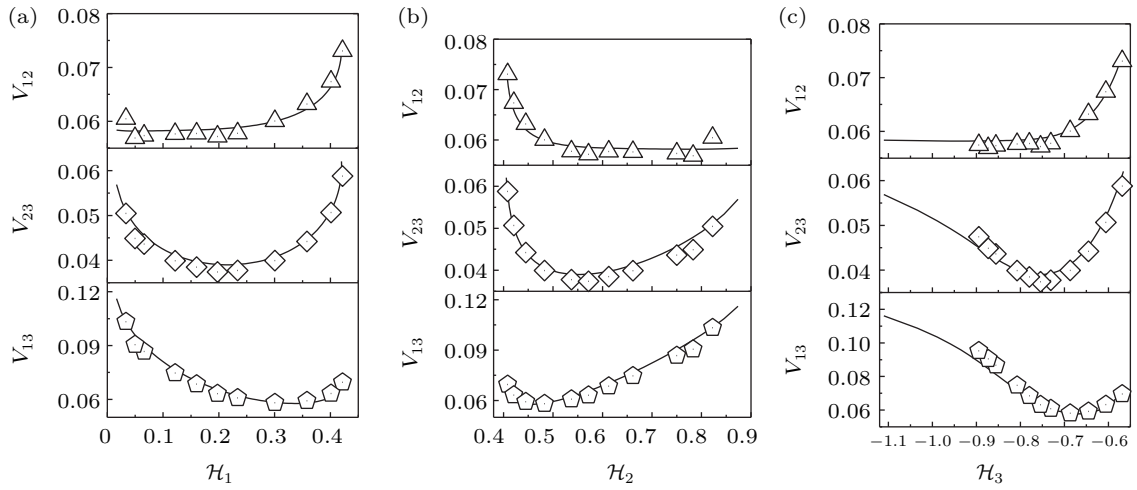


Fig. 4. Normalized covariance $V_{ij} = V_{ji}$ $(i, j = 1, 2, 3;\ j \neq i)$ versus the stability factor $\mathcal{H}_i$. The lines are theoretical predictions according to Eqs. (21)–(23). The hollow markers are from simulations using the Gillespie method.[45,46] Other parameter values are given in the text. All the parameters are measured in hour^{-1}.

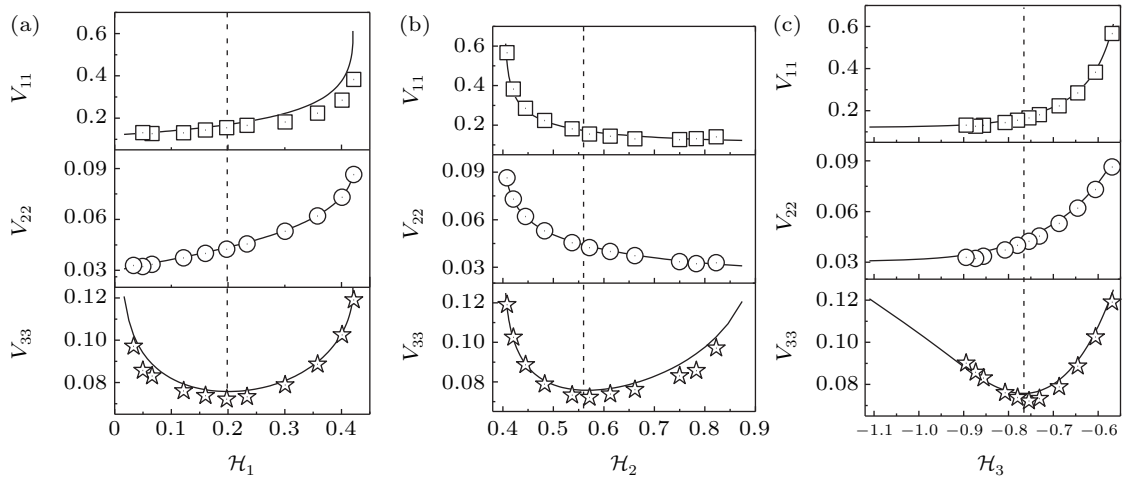


Fig. 5. Noise V_{ii} $(i = 1, 2, 3)$ versus the stability factor $\mathcal{H}_i$. Solid lines are theoretical predictions according to Eqs. (24)–(26). The hollow markers are from simulations using the Gillespie method.[45,46] Dashed lines are auxiliary lines. Other parameter values are given in the text. All the parameters are measured in hour^{-1}.

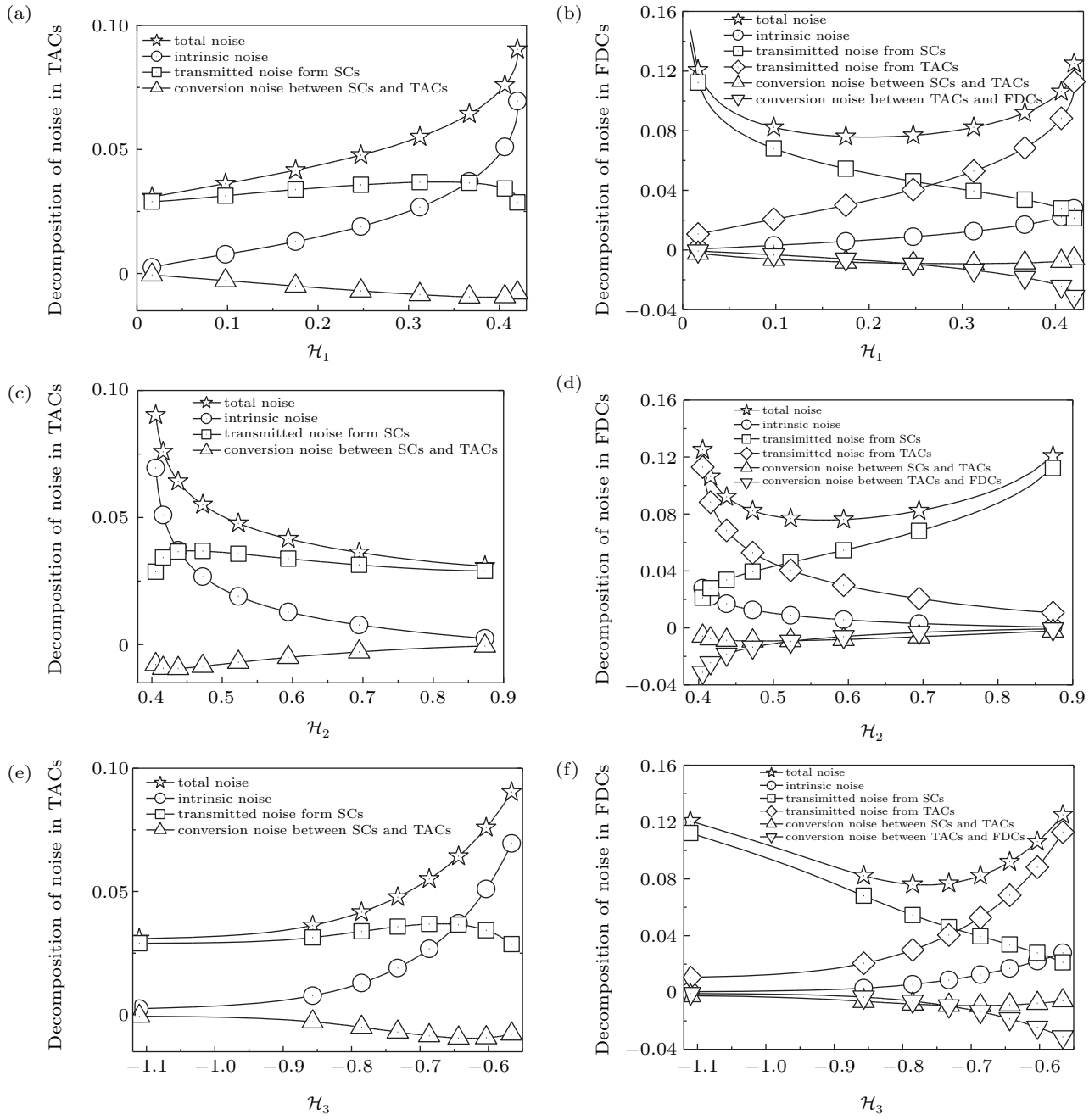


Fig. 6. Noise decomposition versus the stability factor $\mathcal{H}_i$. The lines are theoretical predictions according to Eqs. (25)–(26). Other parameter values are given in the text. All the parameters are measured in hour^{-1}.

4.3. Effects of the stability factor on the noise

By using Eqs. (24)–(26), we can get the effects of the stability factor $\mathcal{H}_i$ on the noise V_{ii} ($i = 1, 2, 3$), as shown in Fig. 5. All analytical predictions are in accord with numerical simulations by the Gillespie stochastic algorithm.

It is found that both V_{11} and V_{22} are monotonically increasing functions of regulation intensity $\mathcal{H}_1$ and $\mathcal{H}_3$, and they are monotonically decreasing functions of H_2. Thus, with the increase in $\mathcal{H}_1$ or $\mathcal{H}_3$, the total noise in SCs and in TACs will increase, and with the increase in $\mathcal{H}_2$, they will decrease. The curves of V_{33} are asymmetric parabolas opening upwards. Therefore, the total noise in FDCs always has a minimum value for some optimal regulation intensities.

From Table 1, we can see that larger $\mathcal{H}_1$ and $\mathcal{H}_3$ values help maintain cell equilibrium. However, the larger values of $\mathcal{H}_1$ and $\mathcal{H}_3$ will cause the total noise in TACs V_{22} to be very large, see the middle layers in Figs. 5(a) and 5(c). Then, the instantaneous number of TACs will be much larger than its equilibrium number, which may induce colon cancer. Therefore, to meet the high stability and low noise requirements of TACs, $\mathcal{H}_1$ and $\mathcal{H}_3$ should take intermediate values. For $\mathcal{H}_2$, its smaller value will not only cause larger noise in TACs V_{22}, but also reduce the cell's stability; see the middle layer in Fig. 5(b). So, a slightly larger $\mathcal{H}_2$ value will be beneficial.

For any $\mathcal{H}_i$, there is an intermediate value (indicated by the dashed line) to minimize the total noise of FDCs V_{33}; see

the three lower layers in Fig. 5. By comparing V_{11}, V_{22}, and V_{33} in the same figure, we find that the intermediate value of $\mathcal{H}_i$ (indicated by the dashed line) may also meet the requirements for the high stability and low noise of TACs. Therefore, the value of $\mathcal{H}_i$ corresponding to the minimum noise in FDCs may be the best choice to enable colon cells to maintain the high stability and low noise of the cascade.

4.4. Effects of the stability factor on the noise propagation

According to Eq. (25), the total noise in TACs can be decomposed into three parts: the intrinsic noise, the transmitted noise from SCs, and the inter-conversion noise between SCs and TACs, as shown in Figs. 6(a), 6(c), and 6(e). According to Eq. (26), the total noise in FDCs can be decomposed into five parts: the intrinsic noise, the transmitted noise from TACs, the transmitted noise from SCs, the inter-conversion noise between TACs and FDCs, and the inter-conversion noise between SCs and TACs, as shown in Figs. 6(b), 6(d), and 6(f). All analytical predictions are in accord with numerical simulations by the Gillespie stochastic algorithm.

From the three figures on the left, we find the conversion noise between SCs and TACs is relatively small and can be omitted. The total noise in TACs V_{22} is mainly determined by its intrinsic noise and the transmitted noise from SCs. With the increase in $\mathcal{H}_i$, the change in the transmitted noise from SCs is relatively small. Then, the change in V_{22} is consistent with that of the inherent noise.

From the three figures on the right, we find the intrinsic noise and the two conversion noises are relatively small and can be omitted. The total noise in FDCs V_{33} is mainly determined by two transmitted noises from TACs and SCs. With the increase in $\mathcal{H}_1$ and $\mathcal{H}_3$, the transmitted noise from SCs is decreasing, and the transmitted noise from TACs is increasing, resulting in the total noise in FDCs first decreasing and then increasing. In contrast, with the increase in $\mathcal{H}_2$, the transmitted noise from SCs is increasing, and the transmitted noise from TACs is decreasing, also resulting in the total noise in FDCs decreasing first and then increasing.

Shortly, the total noise in the source cell only includes intrinsic noise. For the downstream cell, if it can proliferate itself, the total noise is mainly determined by its intrinsic noise and the transmitted noise from upstream cells, and its intrinsic noise is dominant; if it cannot self-proliferate, the total noise is mainly determined by transmitted noises from upstream cells, and with the stability factor increasing, one transmitted noise increases and the other decreases, resulting in a minimum value of the total noise.

5. Discussion and conclusions

Noise is inevitable and plays a constructive role in various biological processes. Whether it is at the gene level or at the cell level, the propagation of noise is confirmed. Maintaining the stability of cell population homeostasis is another key issue.

In a unidirectional phenotypic transition cascade of colonic cells, there are three compartments: SCs, TACs, and FDCs. SCs can differentiate into TACs, and their differentiation rate is regulated by saturated feedback; TACs can differentiate into FDCs, and their differentiation rate is regulated by linear feedback.

The stability factor is introduced into the colon cells cascade, and the influence of the stability factor on noise propagation is studied according to the noise propagation formulas. It is found that the value of the stability factor corresponding to the minimum noise in FDCs may be the optimal choice to enable colonic cells to keep the high stability and low noise of the cascade. Moreover, the total noise in the source cell only includes intrinsic noise. For the downstream cell, if it can proliferate itself, the total noise is mainly determined by its intrinsic noise and the transmitted noise from upstream cells, and its intrinsic noise is dominant; if it cannot self-proliferate, the total noise is mainly determined by transmitted noises from upstream cells, and with the stability factor increasing, one transmitted noise increases and the other decreases, resulting in a minimum value of the total noise.

All analytical predictions in this work are consistent with the numerical simulations by the Gillespie stochastic algorithm.[45,46] It is difficult to quantitatively compare our theoretical results with biological experiments or medical clinical observations, because we only found a small amount of experimental data involving the number of SCs in vivo. Moreover, different experimental groups use different experimental protocols, so the number of SCs obtained is also different. In addition, we have not found real data on the number of TACs and FDCs in published papers up to now.

Noise propagation in colon cells has been studied in our two recent papers. In Ref. [24], pure saturation feedback was used to regulate colon cell differentiation. Taking the upstream cells as input signals and the downstream cells as output signals, noisy signal propagation and amplification were studied. In Ref. [51], four coupled feedbacks were considered to compare the impacts of different feedbacks on noise and noise propagation of cells. The above works only focused on the noise propagation, but ignored the stability of cell population homeostasis. In this paper, we considered the coupled saturation and linear feedbacks to regulate colon cell differentiation, which is more suitable for explaining tumor development. Based on the stability factor, the characteristics of noise and noise propagation were studied, and the mechanism of noise propagation was analyzed. The results obtained are valuable.

This work applies both stochastic dynamics theory and nonlinear dynamics theory to the study of the noise propaga-

tion mechanism, which will provide a new theoretical idea for maintaining the homeostasis of cells in living systems, thereby preventing tumor growth. However, we only considered saturation feedback and linear feedback because, so far, we have not found other feedback that can maintain colon cell homeostasis. Although the form of noise decomposition is the same, different feedbacks will directly affect the value of the stability factor, thereby affecting the characteristics of total noise. Finding other feedback to study the mechanism of noise propagation will be one aspect of our future work. In addition, this transitional cascade of colon cells contains only three phenotypes, and it is unidirectional. If there are more phenotypes in the cascade or the transition between cells is bidirectional, what will happen? This will be another aspect of our future work, and there may be many interesting results.

References

[1] Gui R, Li Z H, Hu L J, Cheng G H, Liu Q, Xiong J, Jia Y and Yi M 2018 *Chin. Phys. B* **27** 028706
[2] Hilfinger A, Norman T M and Paulsson J 2016 *Cell Syst.* **2** 251
[3] Tsimring L S 2014 *Rep. Prog. Phys.* **77** 026601
[4] Raj A and van Oudenaarden A 2008 *Cell* **135** 216
[5] Eldar A and Elowitz M B 2010 *Nature* **467** 167
[6] Zhang N, Zhang H, Liu Z, Ding X, Yang M, Gu H and Ren W 2009 *Chin. Phys. Lett.* **26** 110501
[7] Li Y, Zhang H, Wei C, Yang M, Gu H and Ren W 2009 *Chin. Phys. Lett.* **26** 030504
[8] Ge M, Lu L, Xu Y, Mamatimin R, Pei Q and Jia Y 2020 *Chaos Soliton. Fract.* **133** 109645
[9] Liu Y, Ma J, Xu Y and Jia Y 2019 *Int. J. Bifurcat. Chaos* **29** 1950156
[10] Xu Y, Jia Y, Wang H, Liu Y, Wang P and Zhao Y 2019 *Nonlinear Dynam.* **95** 3237
[11] Cheng G, Gui R, Yao Y and Yi M 2019 *Physica A* **520** 361
[12] Xu Y, Liu M, Zhu Z and Ma J 2020 *Chin. Phys. B.* **29** 098704
[13] Yu H, Meng Z, Liu C, Wang J and Liu J 2021 *Chin. Phys. B* **30** 038703
[14] Zhang Y, Zhou P, Yao Z and Ma J 2021 *Pramana J. Phys.* **95** 49
[15] Ma J, Xu W, Zhou P and Zhang G 2019 *Physica A* **536** 122598
[16] Liu Y, Xu Y and Ma J 2020 *Commun. Nonlinear. Sci. Numer. Simulat.* **89** 105297
[17] Wu F, Ma J and Ren G 2018 *J. Zhejiang Univ. Sci. A* **19** 889
[18] Zhang J, Yuan Z and Zhou T 2009 *Phys. Biol.* **6** 046009
[19] Wang Z and Zhang J 2011 *Proc. Natl. Acad. Sci. USA* **108** E67
[20] Pedraza J M and van Oudenaarden A 2005 *Science* **307** 1965
[21] Baraskar A A, Deb A and Viswanathan G A 2013 *IFAC Proc. Vol.* **46** 89
[22] Kleijn I T, Krah L H J and Hermsen R 2018 *PLoS Comput. Biol.* **14** e1006386
[23] Pei Q M, Zhan X, Yang L J, Shen J, Wang L F, Qiu K, Liu T, Kirunda J B, Yousif A A M, Li A B and Jia Y 2015 *Phys. Rev. E* **92** 012721
[24] Hou X F, Zhou B Q, Zhou Y F, Apata C O, Jiang L and Pei Q M 2020 *Phys. Rev. E* **102** 062411
[25] Boukal Y, Zasadzinski M, Darouach M and Radhy N E 2018 *Mathematical Techniques of Fractional Order Systems* (Advances in Nonlinear Dynamics and Chaos (ANDC)) (Netherlands: Elsevier) pp. 133–158
[26] Chicone C 2012 *Mathematics of Complexity and Dynamical Systems* (New York: Springer) pp. 1653–1671
[27] Niu L, Chen Y, Shen X and Xu T 2020 *Chin. Phys. B* **29** 087803
[28] Ai D, Qiao H, Zhang S, Luo L, Sun C, Zhang S, Peng C, Qi Q, Jin T, Zhou M and Xu X 2020 *Chin. Phys. B* **29** 090601
[29] Noor N A, Mushahid N, Khan A, Kattan N A, Mahmood A and Ramay S M 2020 *Chin. Phys. B* **29** 097101
[30] Guo H, Cheng T and Li Y 2020 *Chin. Phys. B* **29** 115202
[31] Song X, Li B and Xie L 2020 *Chin. Phys. B* **29** 086201
[32] Liu H, Li S, Wang H and Li G 2017 *Chin. Phys. B* **26** 030504
[33] Zhu L and Wang B 2020 *Inform. Sciences* **526** 1
[34] Annas S, Pratama M I, Rifandi M, Sanusi W and Side S 2020 *Chaos Soliton. Fract.* **139** 110072
[35] Boukhouima A, Lotfi E M, Mahrouf M, Rosa S, Torres D and Yousfi N 2021 *Eur. Phys. J. Plus* **136** 103
[36] Allali K 2021 *Biosystems* **199** 104321
[37] Johnston M D, Edwards C M, Bodmer W F, Maini P K and Chapman S J 2007 *Proc. Natl. Acad. Sci. USA* **104** 4008
[38] Pei Q, Zhan X, Yang L, Bao C, Cao W, Li A, Rozi A and Jia Y 2014 *Phys. Rev. E* **89** 032715
[39] Tang N, Yang X Y, Song L, Zhang J, Li X L, Zhou Z K and Shi Y R 2020 *Acta Phys. Sin.* **69** 010301 (in Chinese)
[40] Duan L, Liu C, Zhao L C and Yang Z Y 2020 *Acta Phys. Sin.* **69** 010501 (in Chinese)
[41] Wang W, Deguchi Y, He Y S and Zhang J Z 2019 *Acta Phys. Sin.* **68** 234303 (in Chinese)
[42] Kim K H, Hong Q and Sauro H M 2013 *J. Chem. Phys.* **139** 144108
[43] Pedraza J M and van Oudenaarden A 2005 *Science* **307** 1965
[44] Paulsson J 2004 *Nature* **427** 415
[45] Gillespie D T 1977 *J. Phys. Chem.* **81** 2340
[46] Ni M, Wang S and Ouyang Q 2008 *Chin. Phys. Lett.* **25** 2702
[47] Oyarzún D A, Lugagne J and Stan G V 2015 *ACS Synth. Biol.* **4** 116
[48] Brett T and Galla T 2013 *Phys. Rev. Lett.* **110** 250601
[49] VanKampen N G 2010 *Stochastic Processes in Physics and Chemistry* 3rd edn. (Beijing: World Book Publishing Company Beijing Company) pp. 219–240
[50] Xiong L, Ma Y and Tang L 2010 *Chin. Phys. Lett.* **27** 098701
[51] Zhou B, Apata C O, Zhou Y, Jiang L and Pei Q 2022 *Physica A* **585** 126429